REYNOLDS STRESS MEASUREMENTS ON A PROLATE SPHEROID

G. Iuso; M. Onorato - Aeropspace Dept., Politecnico di Torino, Torino
S. De Ponte - Aerospace Dept., Politecnico di Milano, Milano
M.S. Oggiano - Fluidynamics Research Centre of CNR, Torino

1.Abstract

Measurements of turbulence quantities in the axisymmetric flow in the boundary layer of a prolate spheroid have been made.

The method used to measure the Reynolds stresses using slanted and normal single hot wires is described and preliminary results are presented and discussed.

I. Introduction

Computational fluid dynamics is becoming an increasingly powerful tool in the aerodynamic design of aerospace systems, owing to improvements in numerical algorithms, geometric modeling, grid generation, physical modeling, and to improvements in supercomputer processing speed and memory.

Although the algorithms have reached a relative state of maturity, turbulence modeling remains the major difficulty for many flow problems. Turbulence modeling seems to be the most important issue for computational fluid dynamics today.

Recognizing this fact, a research program has been established between the experimental sections of the Aerospace Departments of the Politecnico di Torino and the Politecnico di Milano and the Centro Studi sulla Dinamica dei Fluidi del CNR, in order to contribute to turbulence modeling. The activities are mainly concentrated on the experimental side of the subject.

The main part of the program deals with turbulence measurements in the 2D and 3D turbulent boundary layer on a 1:6 prolate spheroid at zero angle of attack and at incidence.

The reasons of selecting a prolate spheroid for the experiments are the simplicity of this geometry, its shape close to airplane fusolage and the data already available on mean quantities, velocity profiles and wall shear stress distributions, provided by the present authors [1,2] and, more extensively, by Meier and Kreplin experiments [3,4].

In this paper the experimental procedure will be described and the results of preliminary measurements of the Reynolds stresses in the axisymmetric boundary layer of the model at zero incidence will be shown.

Wall normal and tangential stresses and mean velocity boundary layer profiles will be also reported.

II. Model and Experimental Arrangements

A 1:6 prolate spheroid mould has been made in order to produce as many models are needed for the tests. For the present experiments two models have been used: one equipped with pressure taps and wall shear stress probes, another equipped with pitot tubes and hot wires probes for boundary layer survey.

Table I

Wall stress measur. points	X/L	Φ
1	.139	200°
2	.223	215°
3	.309	230°
4	.395	245°
5	.493	260°
6	.565	275°
7	.652	290°
8	.738	305°
9	.825	320°
10	.883	335°

The models were mounted in the 3 meter diameter test section of the Politecnico di Torino wind tunnel by means of an axial sting which could be rotated around the body axis by a stepper motor device.

In Fig.1 and in Tables I and II, the model, the reference axis, the location of the wall stress measurement points and the location of the boundary layer survay stations are shown.

Table II

Boundary layer survay stations	X/L	Φ
1	.309	91°
2	.493	132°
3	.652	150°

The wall tangential shear stresses were measured by means of Preston tubes, mean velocity profiles and Reynolds stress profiles respectively by Pitot tubes and single hot wires. Reynolds stresses were measured only in station 1.

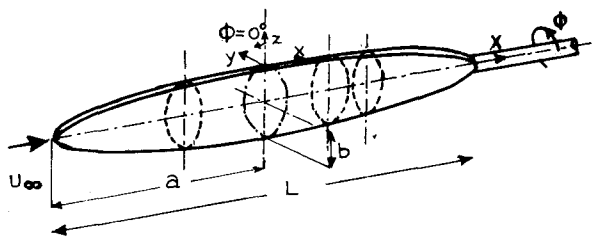

Fig.1 - Model and coordinate system

Boundary layer probes were connected to three transversing devices placed inside the body at the stations indicated in Table II. The single hot wire probe was also allowed to rotate around its axis for the Reynolds stress measurements. The rotating mechanism was located inside the model. Both the transversing and the rotating devices were controlled by computer.

All pressure probes and hot wires were previously calibrated: hot wire calibrations were repeatedly controlled during the tests.

Single hot wire probes were used rather than 3 wire probes due to the unacceptable dimension of the last ones for boundary layer measurements

III. Hot Wire Data Reduction

The method of analysing the hot wire signals, in order to obtain the components of the Reynolds stress tensor, was a conventional one, based on the assumption that triple and higher order turbulence correlations are negligible compared with double correlations[5,6]. The method is here shortly outlined.

The starting point is the response equation relating the hot wire signal to the flow velocity components.

For a wire in the plane parallel to the model surface in the measurement station, the equation is given by

$$E/S = \left\{\left[(\bar{U}+u)\cos\alpha + v\sin\alpha\right]^2 + h^2w^2 + k^2\left[v\cos\alpha - (\bar{U}+u)\sin\alpha\right]^2\right\}^{1/2} \quad (1)$$

where, $\bar{U}$ is the mean velocity in the direction of the model meridian, u, v, w are the components of the fluctuating velocity; u is parallel to the model meridian, v and w are perpendicular to the model meridian, respectively parallel and normal to the body surface; α is the angle between the mean flow direction and the normal to the wire; k and h are the yaw and pitch factors determined by the probe directional calibration, E is the instant electrical linearised output from the hot wire anemometer and S is the sensitivity factor to be determined from the calibration of the probe.

In order to obtain statistical values, equation (1) must be time averaged; this is possible only when the square root in the equation is expanded into a series. Neglecting terms above a certain order, an approximate equation may be written for E/S. Time averaging this equation and putting $e = E - \bar{E}$, where $\bar{E}$ is the mean signal value, it may be obtained

$$\bar{E}/S = \bar{U}\cos\alpha\,(1 + \tan^2\alpha\cdot k^2/2) \quad (2)$$

$$\overline{e^2}/s^2 = \cos^2\alpha\left[\overline{u^2}(1+k^2\tan^2\alpha) + 2\overline{uv}\cdot\tan\alpha(1-k^2) + \overline{v^2}\tan^2\alpha\left[1 - 2k^2(1+(\tan^2\alpha)/2)\right]\right] \quad (3)$$

In equation (2) all fluctuating terms have been neglected, in equation (3) triple and higher order correlations have been neglected. This approximation is suitable if the turbulence level is less than 20 %.

The main velocity may be directly obtained by eqation (2). In order to obtain a system soluble for $\overline{u^2}$, $\overline{v^2}$ and $\overline{uv}$, the signal $\overline{e^2}$ (the square of the RMS value) must be measured at three different angles α. The usual choise is: $\alpha = +45°$, $\alpha = -45°$ and $\alpha = 0°$. In the present experiments the first two conditions have been obtained by a 180° rotation of a DANTEC P12, 45°-slanted, hot wire probe, the last using a DANTEC P11 normal hot wire probe.

Positioning the wire in a plane normal to the model surface, and following the same procedure, $\overline{w^2}$ and $\overline{uw}$ may be obtained.

From the directional calibration of the hot wire probes come out that the best values of h and k that fit equation (1) with experimental data are very close to the typical values found in the literature. We used h = 1 and k = 0.2

IV. Results and Comments

Experiments have been conducted at a Reynolds number of $3x10^6$, based on the major axis of the spheroid and on the wind tunnel velocity of 30 m/s. The turbulence intensity of the freestream was of the order of 0.3 %. Natural transition occurred on the model upstream of station 1. This may be seen from Fig.2, reporting the RMS signal from a normal hot wire, placed in station 1, as function of the free stream velocity and showing that transition occurs in the measurement section at a lower speed of about 20 m/s.

In Fig.3 the pressure coefficient distribution along the model meridian is shown. The flow appears to be completely attached to the body except in the very rear region where the sting supporting the model is present.

It may be seen from Fig.3 that in station 1, where the Reynolds stress measurements have been made, the pressure gradient is about equal to zero.

In Fig.4 the distribution of the skin friction coefficient along the model meridian is reported. It is confirmed that the boundary layer is turbulent in all measurement sections.

The result in Fig.4 can not be compared with the measurements of Meier and Kreplin[7], performed in the DNW wind tunnel, because in their experiments at a Reynolds number of $3x10^6$, the flow is laminar along about all the model. This is due to the different turbulence characteristics of the two tunnels. Further studies are needed to asses these transitional problems.

In Figs.5, 6 and 7 the boundary layer mean velocity profiles in the three stations indicated in Table II are displayed. In Fig.8 the growth of the displacement and momentum thickness and the shape factor are shown. These results and the ones already published by the present authors[1,2], for the case of the same model at an incidence of 14°, are usefull as data for boundary layer numerical methods validation.

Finally in Figs.9,10,11 and 12 the profiles of four of the six components of the Reynolds stress tensor, $\overline{u^2}$, $\overline{w^2}$, $\overline{v^2}$ and $-\overline{uw}$ are reported (the density is omitted being constant). In station 1, where the measurements have been performed, the Reynolds number based on the local boundary layer thickness δ has the value $Re_\delta = 1.03x10^4$ and the ratio between the shear velocity $u_\tau = \sqrt{\tau_w/\rho}$ and the external velocity $\overline{U}_e$ has the value $u_\tau/\overline{U}_e = 0.04$

Although the main object of the measurements was to test the experimental procedure and the method of analysis of the signals, the results are rather interesting, being most of the existing Reynolds stress data referred to boundary layers on flat wall with imposed pressure gradients. Due to the axisymmetric nature of the model, in the present experiments effects of streamlines divergence and wall curvature are included.

Looking at the normal shear stresses, $\overline{u^2}$, $\overline{w^2}$, $\overline{v^2}$, it may be noticed that the intensities of the three turbulence velocities differ appreciably from one another over the main inner part of the boundary layer. The degree of anisotropy increases toward the wall, where the intensity of the axial turbulence component, $\overline{u^2}$, has the highest value. Near

the outer edge $\overline{u^2}$ tends to zero, while $\overline{w^2}$ and $\overline{v^2}$ tend to small non zero values. This may depend on the behaviour of the flow in the irregular and fluctuating region between the boundary layer and the external potential flow, where streamline divergence and curvature effects are present.

The profile of the turbulent shearing stress $-\overline{uw}$ shows a regular behaviour, tending to zero at a distance from the wall corresponding to the boundary layer thickness given by the mean velocity profile. Near the wall its extrapolated value well agrees with the one deduced from the skin friction measurement using the Preston tube.

The presented results refer to a region of the boundary layer that, in natural coordinate zu_τ/ν, is defined between 100 and 400.

From the showed data, the distribution of the turbulent kinetic energy $\overline{q^2}/\overline{U}_e^2$ across the boundary layer has been calculated. The result is shown in Fig.13, together with the distribution of the turbulence shear stress, $-\overline{uw}$, normalized respect to the square of the wall shear velocity u_τ. Considering the region not to close to the boundary layer external edge, a near similarity between the two quantities may be observed; the ratio of the two distributions, as it may be deduced from Fig.13, remains about constant. Complete similarity, that is a constant ratio between the two quantities, would be obtained if von Karman similarity hypothesis, concerning the structure of turbulence, were true. Moreover, according to the von Karman hypothesis, the correlation coefficient, between the longitudinal and transvere fluctuation $\overline{uw}/(\sqrt{\overline{u^2}}\cdot\sqrt{\overline{w^2}})$, is expected to be constant. This is not tha case of the present measurements, where the correlation coefficient ranges over values up to -0.7, as it may be seen in Fig.14.

From the turbulent shear stress distribution and the mean velocity distribution, the eddy viscosity ε_m, across the boundary layer, may be calculated. The results are shown in Fig.15. Unfortunately the measurement point nearest to the wall is at about $z/\delta = 0.3$, therefore the expected linear variation with distance of the wall of the eddy viscosity near the wall may not be checked. Probably in correspondence of the first measurement point $z/\delta = 0.3$, the eddy viscosity, in normalized form, has attained its maximum value, that is $\varepsilon_m/u_\tau\delta = 0.07$.

The fact that, the velocity gradient of the external potential flow, in station 1, is about zero, suggested to compare the present results with flat plate at zero incidence boundary layer results. In the next figures comparisons with Klebanoff[8] data will be shown. The results in Ref.(8) were obtained at Reynolds number, $Re_\delta = 7.5\times10^4$, about seven times higher than in the present results, but at about the same value of the ratio $u_\tau/\overline{U}_e = 0.04$.

Fig.16 shows that a very good agreement is found for $\sqrt{\overline{u^2}}/\overline{U}_e$ and for $\overline{uw}/\overline{U}_e^2$. In the same figure the mean velocity profiles are also reported, showing that the comparisons are made in condition of very similar mean velocity distribution across the boundary layer. The square symbol, for $z/\delta = 0$, refers to the wall shear stress measured on the prolate spheroid with Preston tube.

This agreement is completely lost if we compare the $\sqrt{\overline{v^2}}/U_e$ and $\sqrt{\overline{w^2}}/U_e$ components, as it is demonstrated in Figs.17 and 18. Except in the outer part of the boundary layer, where in the present experiment $\overline{v^2}$ and $\overline{w^2}$ don't reach the zero value, the results on the prolate spheroid show a lower value respect to the flat plate case.

To explain this behaviour further experiments are needed. Certainly a different behaviour of the turbulence in the flat plate case and in the present axisymmetric case must be expected. The boundary layer on the prolate spheroid is subjected to the streamlines divergence effects and to the body wall longitudinal and transversal curvature effects. Moreover even if the two compared boundary layers show locally a similar behaviour for the mean quantities, the upstream boundary layer histories are different. The flow for the prolate spheroid is accelerated from the rest to the conditions in the measurement station, on the contrary the flow along the flat plate develops under zero pressure gradient.

In order to better understand the turbulent flow under study, the spectrum of

the axial turbulent velocity u at a given distance from the wall is shown in Fig.19, where the flat plate result[8] is also displayed. $E_1(k_1)$ is given by: $E_1(k_1) = E_1(f)\bar{U}_e/2\pi$ where $E_1(f)df = \overline{u^2}$, k_1 is the wavenumber, $k_1 = 2\pi f/\bar{U}_e$, and f is the frequency.

It may be seen that the spectrum for the prolate spheroid follows the -5/3 law in a region of wave-numbers ranging from $k_1 \cong$ 400 to 2000 m^{-1}.

Finally an attempt has been done to compare the measured values of $-\overline{uw}$ with the ones obtained by the algebraic eddy-viscosity formulation developed by Cebeci and Smith, usually adopted in most of boundary layer calculations. Results are shown in Fig.20, where it may be seen that the theoretical results underestimate the behaviour given by the present data for most part of the boundary layer thickness. Probably this may explain the results shown in Ref.(9), where calculated wall shear tangential stresses on a prolate spheroid at incidence of 10°, using Cebeci and Smith formulation, appear to be lower than corresponding experimental data.

V Conclusions

Preliminary measurements of Reynolds stresses in the boundary layer of a prolate spheroid have been shown. The procedure adopted for analysing the hot wire signals seems to be adequate.

The results have been compared both with flat plate experimental results and simple theoretical turbulence model, and some comments are given.

In order to understand better the flow behaviour pointed out by these preliminary results, further experiments are planned. Turbulence measurements will be repeated in the same station at different Reynolds numbers and will be extended in a region farer to the wall. Measurements will be also performed in stations downstream, where the conditions of pressure gradient and the boundary layer thickness are different.

Having turbulence data in different stations, other turbulence model, rather than simple algebraic one, will be compared with experiments.

Acknowledgments

The authors are very grateful to Mr. F. Giovara and Mr. R. Tassone for their technical assistance.

References

1.- G. Iuso; M. Onorato; M.S. Oggiano; S. De Ponte "Experimental Investigation of the complex 3D flow around a body of revolution at incidence. A Sino-Italian cooperative research program" 16th ICAS Congress, Jerusalem (1988)

2. - G. Iuso; M.S. Oggiano; S. De Ponte; B. Yuzhong; Z. Xiaodi "3D Boundary layer measurements on an ellipsoid at angle of attack" Proc. of the ICFM, Beijing (1987)

3. - H.U. Meier; H.P. Kreplin "Experimental investigation of the boundary layer transition and separation on a body of revolution" Z. Flugwiss. Weltraumforsch. 4 (1980), Heft 2

4. - H.P. Kreplin; H. Vollmers; H.U. Meier "Measurements of the wall shear stress on an inclined prolate spheroid" Z. Flugwiss. Weltraumforsch. 6 (1982), Heft 4

5. - W. Rodi "A new method of analysing hot wire signals in highly turbulent flow, and its evolution in a round jet" DISA Information N.17 (1975)

6. - F.H. Champagne; C.A. Sleicher; O.H,Wehrmann "Turbulence measurements with inclined hot-wires" Part.1 and Part.2 , J. of Fluid Mech. Vol.28 (1967)

7. - H.P. Kreplin; H.U.Meier, et al. "Wall shear stress measurements on a prolate spheroid at zero incidence in the DNW wind tunnel" DFVLR Goettingen Rep. (Feb. 1986)

8. - P.S. Klebanoff "Characteristics of turbulence in a boundary layer with zero pressure gradient" NACA Rep. 1247 (1955)

9. - H.U. Meier; T. Cebeci "Flow characteristics of a body of revolution at incidence" 3rd Symp. on Numerical and Phys. Aspects of Aerod. Flows Long Beach - USA (Jan. 1985)

The research has been supported by MURST (Italian Ministry of University and Scientifical Technological Research) and by CNR (Italian National Research Council)

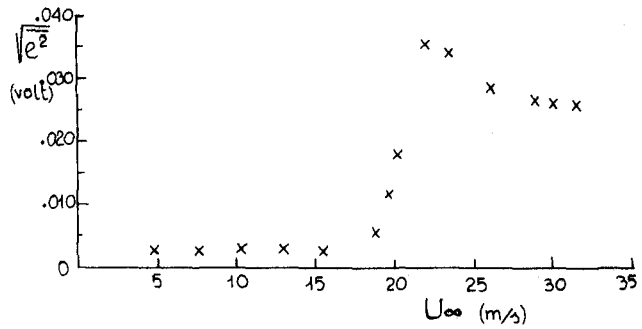

Fig.2 - Transition behaviour in section 1

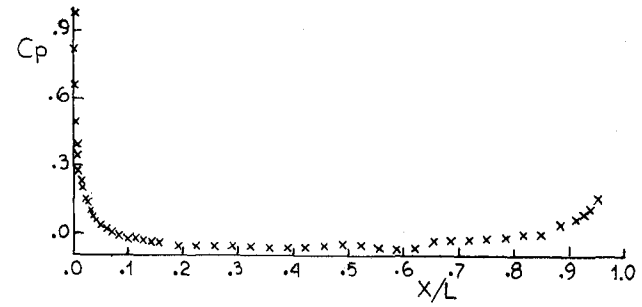

Fig.3 - Pressure coefficient distribution along the model

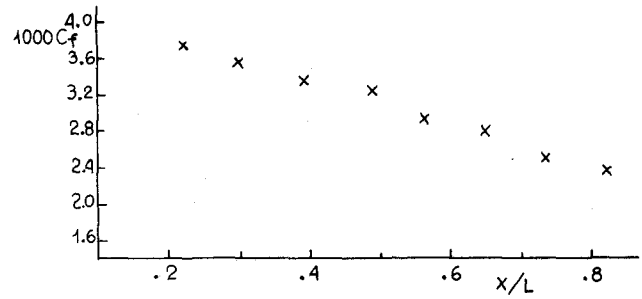

Fig.4 - Skin friction coefficient distribution along the model

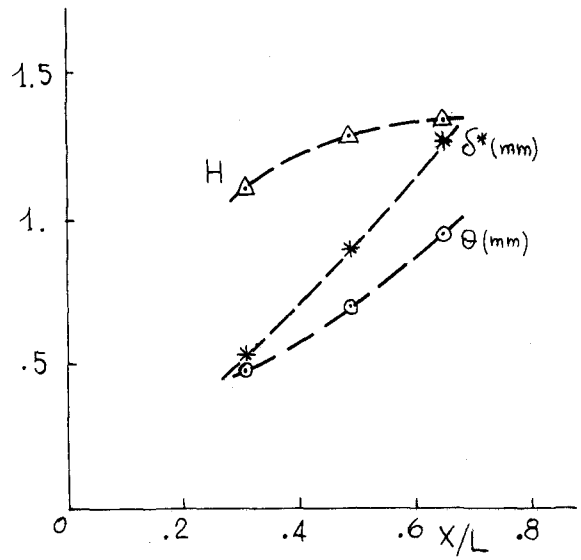

Fig.8 - Boundary layer displacement thickness δ^* momentum thickness θ and shape factor H

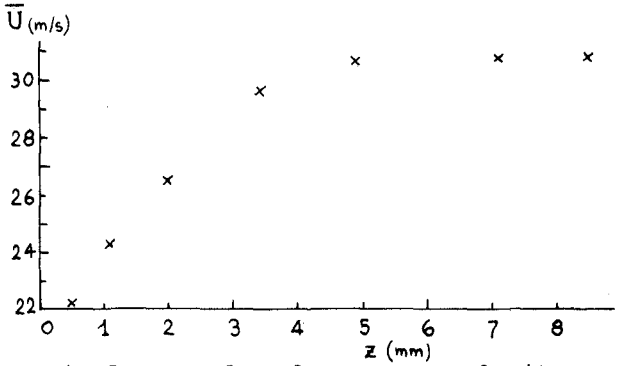

Fig.5 - Boundary layer mean velocity profile in section 1 (X/L=.309)

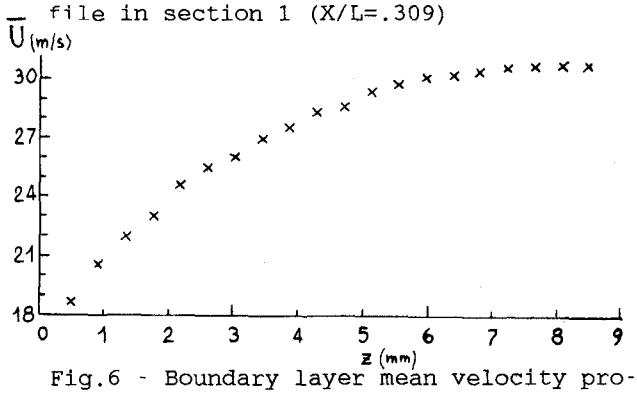

Fig.6 - Boundary layer mean velocity profile in section 2 (X/L=.493)

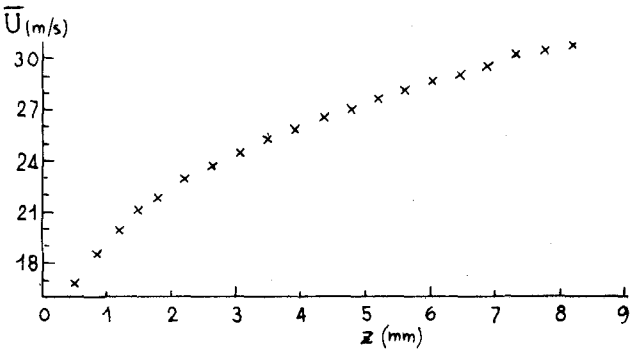

Fig.7 - Boundary layer mean velocity profile in section 3 (X/L=.652)

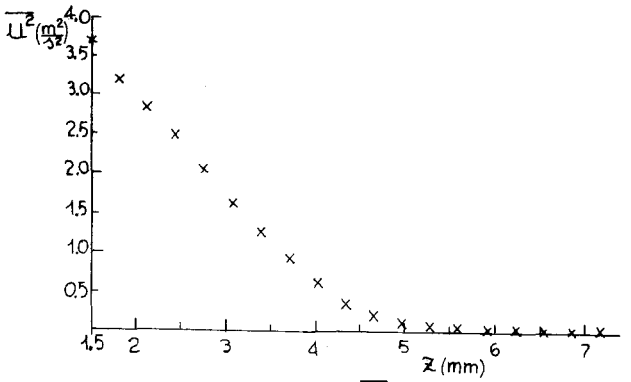

Fig.9 - Boundary layer $\overline{u^2}$ profile (station 1)

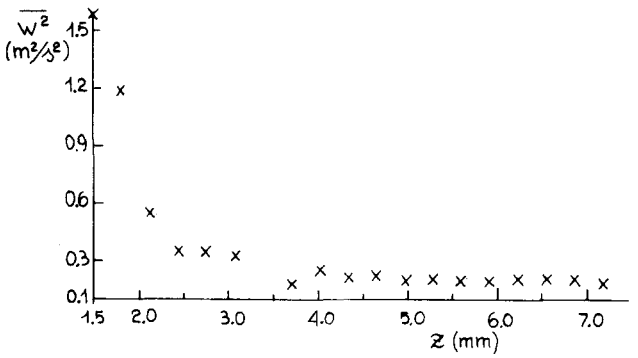

Fig.10 - Boundary layer $\overline{w^2}$ profile (station 1)

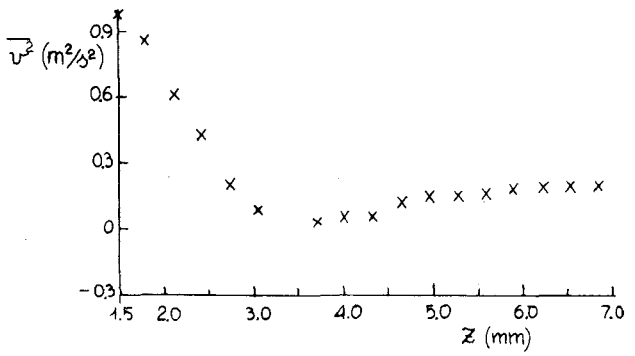

Fig.11 - Boundary layer $\overline{v^2}$ profile (station 1)

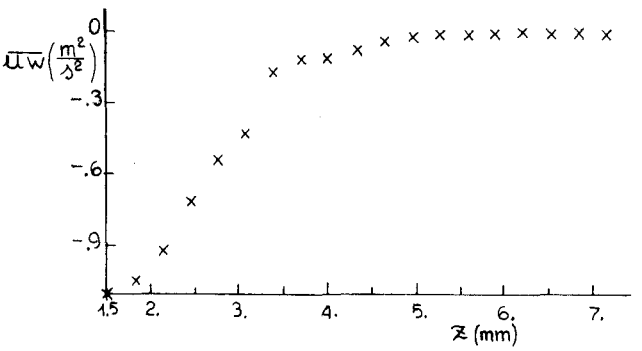

Fig.12 - Boundary layer $\overline{uw}$ profile (station 1)

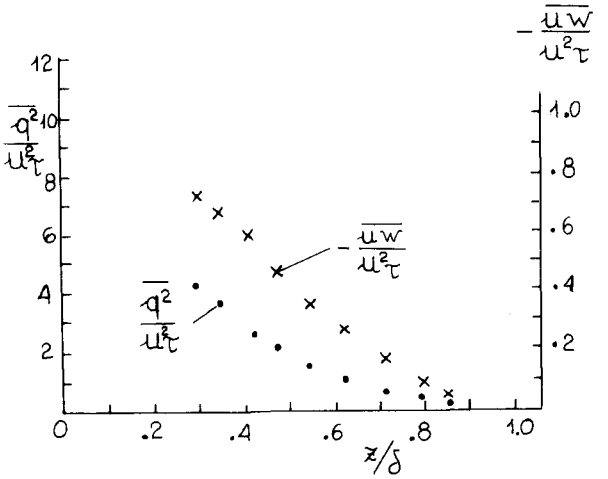

Fig.13 - Distribution of turbulent kinetic energy and turbulent shear stress across the boundary layer (station 1)

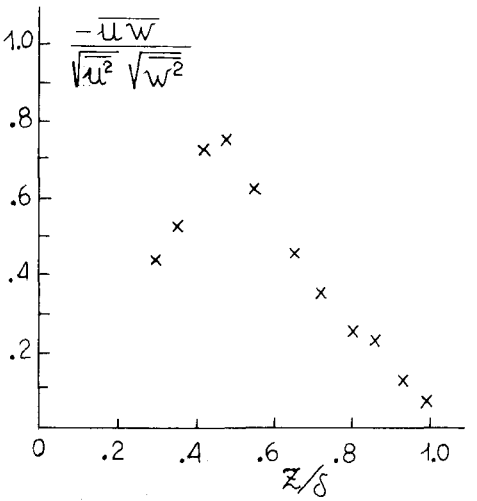

Fig.14 - Correlation coefficient across the boundary layer (station 1)

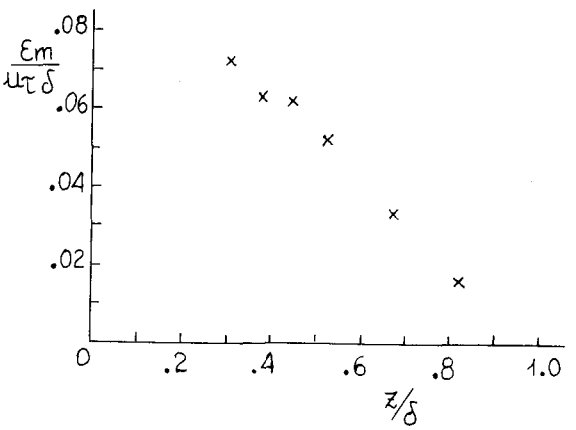

Fig.15 - Distribution of eddy viscosity across the boundary layer (station 1)

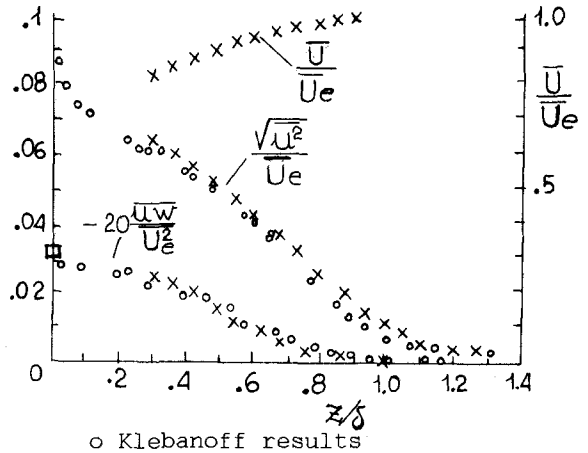

o Klebanoff results

x present results

Fig.16 - Comparison with Klebanoff[8] flat plate results

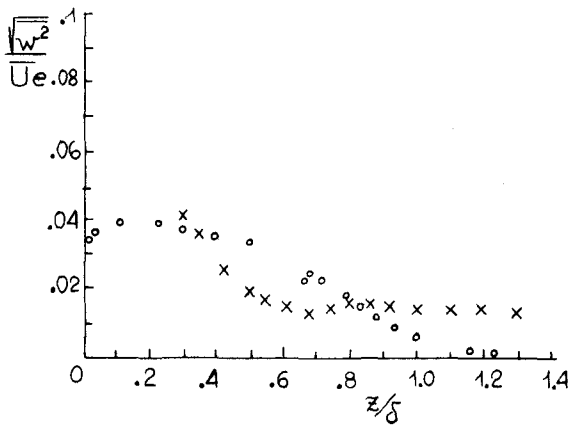

o Klebanoff results

x present results

Fig.17 - Comparison with Klebanoff[8] flat plate results

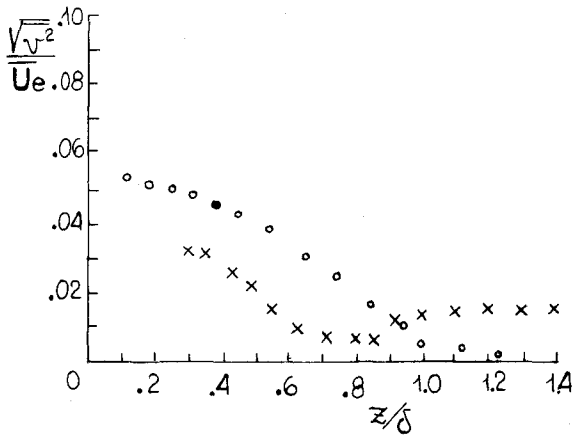

o Klebanoff results

x present results

Fig.18 - Comparison with Klebanoff[8] flat plate results

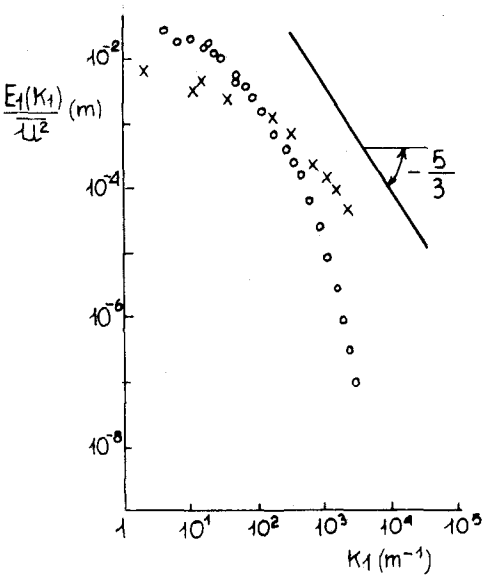

o Klebanoff results

x present results

Fig.19 - Spectrum of u in the boundary layer. Comparison with Klebanoff[8] flat plate results

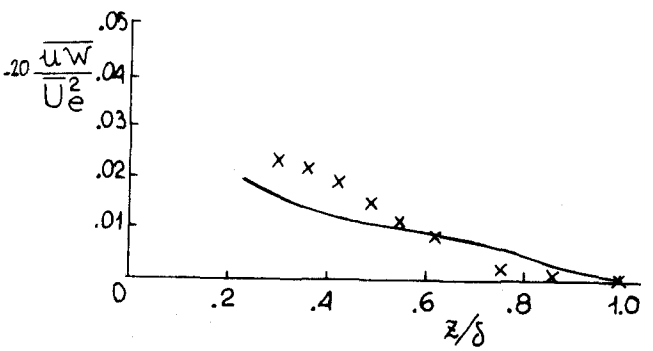

——— Cebeci and Smith formulation

x x x present results

Fig.20 - Comparison between present measurements and theoretical results given by Cebeci and Smith algebraic eddy viscosity formulation